Author Manuscript

Author Manuscript

Author Manuscript

Author Manuscript

HHS Public Access

Author manuscript

ChemMedChem. Author manuscript; available in PMC 2017 May 06.

Published in final edited form as:

ChemMedChem. 2016 May 6; 11(9): 980–989. doi:10.1002/cmdc.201600090.

Acyclic Cucurbit[n]uril-Type Molecular Containers: Influence of Linker Length on their Function as Solubilizing Agents

David Sigwalt[a], **Damien Moncelet**[b], **Shane Falcinelli**[b], **Vijaybabu Mandadapu**[c], **Peter Y. Zavalij**[a], **Anthony Day**[c], **Volker Briken**[b], and **Lyle Isaacs**[a]

Volker Briken: vbriken@umd.edu; Lyle Isaacs: LIsaacs@umd.edu

[a]Department of Chemistry, University of Maryland, College Park, Maryland 20742, United States

[b]Department of Cell Biology and Molecular Genetics, University of Maryland, College Park, Maryland 20742, United States

[c]Department of Chemistry, University of New South Wales Canberra, Australian Defence Force Academy, Canberra, ACT 2600, Australia

Abstract

Two acyclic CB[n]-type molecular containers that differ in the length of the $(CH_2)_n$ (**M2C2**, n=2, **M2C4**, n=4) linker between their aromatic sidewalls and SO_3^- solubilizing groups were prepared and studied. The inherent solubilities of **M2C2** (68 mM) and **M2C4** (196 mM) are higher than the analogue with a $(CH_2)_3$ linker (**M2**, 14 mM) studied previously. ^{1}H NMR dilution experiments show that **M2C2** and **M2C4** do not self-associate in water, which enables their use as solubilizing excipients. We used phase solubility diagrams (PSD) to compare the solubilizing ability of **M2**, **M2C2**, **M2C4**, hydroxypropyl-β-cyclodextrin (HP-β-CD), and sulfobutylether-β-cyclodextrin (SBE-β-CD) toward 15 insoluble drugs. We find that **M2C2** and **M2C4** – as gauged by the slope of their PSDs – are less potent solubilizing agents than **M2**. However, the higher inherent solubility of **M2C2** allows higher concentrations of drug to be formulated using **M2C2** than with **M2** in several cases. The solubilizing ability of **M2C2** and SBE-β-CD were comparable in many cases with K_{rel} values averaging 23 and 12, respectively, relative to HP-β-CD. *In vitro* cytotoxicity and *in vivo* maximum tolerated dose studies document the biocompatibility of **M2C2**.

TOC image

Acyclic cucurbit[n]uril-type molecular containers function as solubilizing excipients for insoluble drugs. The influence of the length of the linker between the aromatic wall and the sulfonate solubilizing group (e.g. **M2C2**, **M2**, **M2C4**) on their inherent aqueous solubility and recognition properties toward insoluble drugs are presented. The **M2C2** does not display significant in vitro cytotoxicity and a maximal tolerated dose study indicates **M2C2** is well tolerated in mice.

Correspondence to: Volker Briken, vbriken@umd.edu; Lyle Isaacs, LIsaacs@umd.edu.

Supporting information for this article is given via a link at the end of the document.

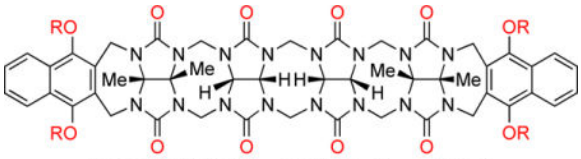

M2C2; **M2**; **M2C4** (R = $(CH_2)_nSO_3Na$; n = 2, 3, 4)

Keywords

Cucurbituril; cyclodextrin; solubilizing excipient; molecular recognition; host-guest chemistry

Introduction

A central topic in the field of supramolecular chemistry is the synthesis of new molecular container compounds, studies of their molecular recognition properties and incorporation into functional systems. The most popular classes of macrocyclic containers include the crown ethers, cyclodextrins, calixarenes, cyclophanes, cucurbiturils, pillararenes, and a variety of receptors created by self-assembly processes.[1] The great interest in host•guest complexes stems from the fact that the properties of free guest and complexed guest (e.g. chemical stability, electrochemistry, conformational preferences, photophysical, pK_a) often differ dramatically. Accordingly, host•guest complexes have been used to stabilize otherwise unstable compounds like white phosphorous (P_4),[2] to catalyze the bowl-to-bowl interconversion of corannulene,[3] to shift the pK_a of included guests (e.g. acetals) and thereby promote hydrolysis reactions under basic conditions,[4] to create chemical sensing ensembles,[5] and to contort alkanes into helical conformations.[6] The supramolecular chemistry of the cucurbit[n]uril (CB[n]) family of molecular containers (Figure 1) is particularly rich, in large part due to their high affinity, high selectivity, and stimuli responsive host•guest complexes.[7] For example, CB[n] compounds function as catalysts for cycloadditions reactions,[8] components of biomembrane and chemical sensing systems,[9] promotors of dimerization assembly for materials and biological applications,[10] and sorption materials for gas purification.[11]

Over the past 20 years, the adoption of combinatorial chemistry tools by pharmaceutical industry has resulted in the rapid generation of new small molecules with good biological activity. Unfortunately, the solubility of an estimated 40–70% of these new chemical entities are so low that they cannot be formulated alone in water.[12] The pharmaceutical industry has responded by developing tools to enable the formulation of these insoluble drugs including nanocrystalline solid forms, solid dispersions, co-solvent systems (e.g. Cremophore), prodrug approaches, co-crystals, and cyclodextrin derived solubilizing excipients (e.g. HP-β-CD and SBE-β-CD; Figure 1).[13] Accordingly, researchers in the CB[n] field are actively investigating their potential in biomedical applications including the solubilization of insoluble drugs,[14] their inherent cytotoxicity both *in vitro* and *in vivo*,[15] their ability to delay or reverse the (side) effects of drugs,[16] for controlled release,[17] and for targeted drug delivery.[18]

Author Manuscript Author Manuscript Author Manuscript Author Manuscript

Author Manuscript Author Manuscript Author Manuscript Author Manuscript

Several years ago, the Isaacs group used our synthetic and mechanistic knowledge of the CB[n] forming reaction[19] to design acyclic CB[n]-type receptors (**M1** and **M2**, Figure 1) that retain many of the essential structural and molecular recognition features of the CB[n] family. Compounds **M1** and **M2** feature a central C-shaped glycoluril tetramer, two terminal aromatic walls, and four sulfonate solubilizing groups. Compound **M1** has very good aqueous solubility (346 mM), dramatically increases the solubility of insoluble drugs, is not toxic when assayed *in vitro* and *in vivo*, and can be used to formulate and deliver albendazole to animals.[20] Previously, we have studied the influence of the solubilizing group (e.g. SO_3Na versus NH_3^+), the identity of the aromatic sidewall (e.g. (substituted) benzene versus (substituted) naphthalene, and the length of the central glycoluril oligomer on their ability as solubilizing agents for insoluble drugs.[21] In brief, we found that **M2** – with its SO_3Na solubilizing groups, a central glycoluril tetramer, and naphthalene walls is the most potent general purpose solubilizing agent. Unfortunately, **M2** is also the least soluble (14 mM) acyclic CB[n]-container in this series which limits the amount of insoluble drug that can be formulated by internal complexation. In this paper, we investigate two new containers (**M2C2** and **M2C4**) that differ from **M2** only in the length of the alkyl chain between the aromatic walls and the SO_3Na groups with the goal of improving the inherent solubility of the host while retaining the excellent recognition properties of **M2**.

Results and Discussion

This results and discussion section is organized as follows. First, we describe the synthesis of the two new containers (**M2C2** and **M2C4**) followed by the determination of their inherent solubility and self-association properties in aqueous solution. Next, we describe the creation of phase solubility diagrams (PSD) with 15 drugs and analyze the trends in the solubilization data. Then, we compare the data obtained with the more promising new host (**M2C2**) with that of SBE-β-CD which is an approved formulation method for several drugs administered to humans. Finally, we present the results of *in vitro* and *in vivo* toxicity studies conducted using **M2C2**.

Design and Synthesis of M2C2 and M2C4

As described previously, the design of acyclic CB[n]-type receptors (e.g. **M2**) is based on the use of a central glycoluril oligomer that imparts a preorganized C-shaped hydrophobic cation binding space with two naphthalene walls bearing four alkyl SO_3Na groups. These compounds have the potential to bind to a wide variety of insoluble aromatic ring containing drugs by π–π interactions, thereby enhancing their aqueous solubility. The preparation of containers **M2C2** and **M2C4** were modeled on the synthesis of **M2**. The naphthalene alkyl-SO_3Na groups were changed to ethyl or butyl to determine which variation would improve aqueous solubility. To prepare the sidewall with the ethyl or butyl-SO_3Na groups, we initially reacted 1,4-dihydroxynaphthalene (**1**) with dibromoethane under basic conditions (K_2CO_3, 18-crown-6, CH_3CN, 70 °C) to give **2** in 40% yield (Scheme 1). Transformation of dibromide **2** into the required $(CH_2)_2SO_3Na$ naphthalene sidewall **3** was accomplished by heating with 2.2 equiv. of Na_2SO_3 in H_2O/DMF (1:1) at 100 °C to give **3** in 81% yield. Treatment of **1** with butanesultone (**4**) under basic conditions (NaOH, H_2O, dioxane) at room temperature gave the required sidewall **5** with the $(CH_2)_4SO_3Na$ groups in 26% yield

Author Manuscript Author Manuscript Author Manuscript Author Manuscript

(Scheme 1). Reaction of **3** (**5**) with glycoluril tetramer bis(cyclic ether) **6** by a double electrophilic aromatic substitution reaction (CF_3CO_2H/Ac_2O (1:1), 70 °C) delivered **M2C2** (**M2C4**) in 58% (43%) yield. **M2C2** and **M2C4** were fully characterized by the standard methods (^1H and ^{13}C NMR, IR, high resolution mass spectrometry) which are in agreement with the depicted C_{2v} symmetric structures.

X-ray Crystal Structure of M2C4

We were fortunate to obtain single crystals of **M2C4** by slow evaporation of an aqueous solution that were suitable for determination of the x-ray crystal structure.[22] Figure 2 shows a cross-eyed stereoview of one molecule of **M2C4** contained within the unit cell. As expected, the methylene bridged glycoluril tetramer imparts an overall C-shape to the molecule and the aromatic naphthalene sidewalls further shape the hydrophobic cavity. As observed previously for **M2**, **M2C4** exhibits a helical twist due to the out of plane splaying of its naphthalene walls; both senses of helicity are present in the crystal.[20a] Unlike **M2**, two of the $O(CH_2)_4SO_3Na$ arms of **M2C4** appear to partially fill their own cavity. Specifically, one Ar-O-CH_2 group on each sidewall is oriented such that the $(CH_2)_4$ group of one wall forms van der Waals interactions with the opposing sidewall and vice versa.[20a] These intramolecular non-covalent interactions would need to be broken in order for **M2C4** to form **M2C4•**guest interactions and will therefore reduce the observed binding constants.

Determination of Inherent Solubility of M2C2 and M2C4

After having completed the synthesis of **M2C2** and **M2C4** we decided to measure the inherent solubility of these new containers in our standard 20 mM sodium phosphate buffered D_2O at pD 7.4. A saturated solution of container was prepared by adding solid **M2C2** or **M2C4** to water until solid container remained undissolved. The insoluble material was removed by filtration and the concentration of **M2C2** or **M2C4** in solution was measured by a ^1H NMR assay employing 1,3,5-benzenetricarboxylic acid as an internal standard of known concentration as described previously.[20a,21a] In this manner we determined the inherent solubilities of **M2C2** and **M2C4** as 68 and 196 mM, respectively. It is worth noting, however, that solutions of **M2C4** higher than 100 mM become increasingly viscous. The high solubility of both **M2C2** and **M2C4** compared to **M2** (14 mM) makes them potentially useful alternatives to **M2** when high concentrations of formulated drug are required.

Containers M2C2 and M2C4 do not undergo strong self-association in water

Previously, we have measured the self-association constant (K_s) of **M2** in 20 mM phosphate buffered D_2O at pD 7.4 as 624 M^{-1} by monitoring the change in chemical shift of the aromatic wall protons as a function of concentration by ^1H NMR spectroscopy and fitting the data to a standard 2-fold self-association model.[21a] We performed related ^1H NMR dilution experiments for **M2C2** (67 mM to 66 μM) and **M2C4** (66 mM to 65 μM) and determined the K_s values to be 6 M^{-1} and 66 M^{-1}, respectively (Supporting Information). More highly concentrated solutions of **M2C4** flow somewhat slowly which suggests they are more viscous than less concentrated solutions. The observed lower intermolecular self-association constants establish that **M2C2** and **M2C4** will exist more fully in their

Author Manuscript Author Manuscript Author Manuscript Author Manuscript

monomeric forms in solution which could enhance their abilities as solubilizing excipients relative to **M2**. However, one must also consider the possibility that the $O(CH_2)_nSO_3Na$ arms can fold into their own cavity in solution as observed in the x-ray crystal structure of **M2C4** (Figure 2). Such a self-folding event would tend to decrease the ability of the container to undergo intermolecular self-association and also decrease the ability to bind to insoluble drugs. Accordingly, we examined the ^{1}H NMR chemical shifts of the $O(CH_2)_nSO_3Na$ arms of containers **M2**, **M2C2**, and **M2C4** relative to the sidewalls **3** and **5** as model compounds for evidence of self-folding. For all three containers the CH_2 groups become diastereotopic so two resonances are seen (Supporting Information). We find that the resonances for the arms of **M2C2** and **M2C4** are shifted slightly farther upfield relative to the sidewall model compounds as compared to **M2**. This suggests that containers **M2C2** and **M2C4** may undergo more significant self-folding phenomena than **M2**.

Theory of Phase Solubility Diagrams

In order to motivate the discussion of the experimentally determined PSDs created with **M2C2**, **M2C4**, and SBE-β-CD it is useful to first discuss PSDs from a theoretical viewpoint.[21a,23] PSDs are plots of the concentration of insoluble drug in solution versus the concentration of container used (Figure 3). PSDs can display a variety of forms, but linear PSDs (known as A_L-type) are common and are taken as evidence that container and drug form soluble well defined complexes of 1:1 stoichiometry.[23] When A_L-type PSDs are observed, the system behaves according to equation 1 which allows for a determination of the binding constant K_a for the container•drug complex based on the experimentally determined slope of the PSD and inherent solubility of the drug (S_0). The slope of the PSD is a measure of the efficiency of solubilization of drug; we consider a container that solubilizes 50 mole percent (e.g. [container] = 100 mM gives [drug] = 50 mM) to be an efficient solubilizing agent. If a slope of 0.5 is inserted into equation 1, then it is easy to demonstrate that $K_a \times S_0 = 1$. Accordingly, if we wish to efficiently solubilize a drug (e.g. slope ≥ 0.5) which has an inherent solubility 10 μM (1 μM) then the container must bind to the drug with a K_a value of at least 10^5 M^{-1} (10^6 M^{-1}). In this context, the generally higher K_a values observed for CB[n]•guest complexes relative to cyclodextrin•guest complexes promises to enable the formulation of drugs of lower inherent solubility. Figure 3 shows calculations of PSDs for a hypothetical container-drug system that obeys equation 1, with an inherent drug solubility of 10 μM and different values of K_a for the container•drug complex. As can readily be seen, increasing (decreasing) the K_a value 9-fold changes the slope of the PSD from 0.5 to 0.9 (0.1) respectively. Conversely, differences in experimentally determined slope can be translated into differences in K_a. In this paper we intend to compare the solubilizing abilities of different containers (e.g. C1 and C2) toward a given drug (D1) so it is also useful to consider equation 2 which relates the slopes of two PSDs to the relative binding constant K_{rel}. Advantageously, a precise knowledge of $S_{o,D1}$ is not required to determine the relative binding constant (K_{rel}) of two different containers toward a given drug since it cancels out on the top and bottom of equation 2.

$$K_a = \frac{\text{slope}}{S_0(1 - \text{slope})} \quad (1)$$

Author Manuscript Author Manuscript Author Manuscript Author Manuscript

$$K_{rel}=\frac{K_{a,C1\cdot D1}}{K_{a,C2\cdot D1}}=\frac{\frac{slope_{C1\cdot D1}}{S_{0,D1}(1-\ slope_{C1\cdot D1})}}{\frac{slope_{C2\cdot D1}}{S_{0,D1}(1-\ slope_{C2\cdot D1})}}=\frac{(slope_{C1\cdot D1})(1-\ slope_{C2\cdot D1})}{(slope_{C2\cdot D1})(1-\ slope_{C1\cdot D1})} \quad (2)$$

Use of M2C2, M2C4, and SBE-β-CD as Solubilizing Agents for Insoluble Drugs

To assess the abilities of the newly synthesized containers **M2C2** and **M2C4** as solubilizing agents for insoluble drugs relative to **M2**, HP-β-CD,[20a,21a] and SBE-β-CD we created PSDs for the containers with 15 insoluble drugs (Figures 4 and 5). Of these 15 drugs, 13 are used in practice whereas PBS-1086[24] and MEPBZ[25] are not in clinical use. We created the PSDs as described previously.[20a,21a] In brief, we stir a known concentration of container with an excess of insoluble drug overnight to establish equilibrium, filter or centrifuge away the excess insoluble drug, and then measure the concentration of drug in solution by ^{1}H NMR integration relative to added 1,3,5-benzenetricarboxylic acid as internal standard of known concentration. In this manner we constructed PSDs for the solubilization of 15 drugs with **M2C2** and SBE-β-CD and a subset of these drugs with **M2C4** due to limitations discussed below (Supporting Information). In most cases, the newly measured PSD are linear at low container concentration, which is consistent with well defined 1:1 complexes. Table 1 presents the results of these studies including the inherent solubility of the drug (S_0), the slope of the PSD, the K_{rel} value referenced to the weakest binding container (generally HP-β-CD), and K_a values. The values for **M2** and HP-β-CD measured previously[20a,21a] under identical conditions are also presented in Table 1 for comparison. The uncertainty in K_a and K_{rel} values are generally ≤ 24%, as derived from the error in the linear regression fitting of the slope of the PSD, although larger uncertainties are noted for PSDs with slope approaching unity which leads to large errors in the (1 – slope) terms of equations 1 and 2 (Supporting Information).

Container M2C4 forms Gels with Insoluble Drugs—Given that **M2** is an excellent receptor and solubilizing agent for steroids,[21a,26] we decided to first create PSDs for **M2C2** and **M2C4** with estradiol (Figure 4a). As can be seen, both **M2C2** and **M2C4** are excellent solubilizing agents for estradiol with slopes of 0.67 and 0.59 at lower concentrations of containers, respectively. **M2C2** (68 mM) is capable of solubilizing 45 mM estradiol. For concentrations of **M2C4** above 32 mM, the amount of estradiol solubilized plateaus at ≈ 20 mM. The presence of a plateau region in PSDs indicates the formation of container•drug complexes of limited solubility.[23] In addition, when concentrations of **M2C4** above 100 mM were used as a solubilizing agent for estradiol we observed the formation of gels. Similarly, the use of concentrations of **M2C4** greater than 16 mM lead to the formation of gels when used as a solubilizing agent for amiodarone. Figure 4b shows the PSDs created for voriconazole. In this case, both **M2C2** and **M2C4** solubilize voriconazole efficiently with slopes of 0.89 and 0.85, respectively, with no evidence of gel formation at 68 mM container. Given the comparable PSD slopes for **M2C2** and **M2C4** at low concentrations and the observation of gels with **M2C4** at higher concentrations – which are not appropriate for use as a solubilizing excipient – we decided to limit our studies of the remaining 12 drugs to **M2C2** as a solubilizing agent.

Author Manuscript Author Manuscript Author Manuscript Author Manuscript

Solubilizing Ability of M2C2 relative to M2—In a previous study of five acyclic CB[n]-type containers with different aromatic walls, we found that the **M2** container often displayed the highest slope and K_a values toward the insoluble drugs.[20a,21a] As noted above, the maximum solubility of **M2C2** (68 mM) is significantly higher than that of **M2** (14 mM) which could translate into the ability to prepare formulations containing higher drug concentrations if the K_a values of **M2C2** and **M2** toward a given drug are equal. An examination of Table 1 reveals that **M2** is the superior solubilizing agent (e.g. higher slope and K_a) in all cases. In some cases the difference in slope is small (e.g. 0.31 vs. 0.28 for aripiprazole) whereas in other cases the difference is substantial (e.g. 0.54 vs. 0.11 for tolfenamic acid). The K_a values for the 15 drugs toward **M2** (**M2C2**) range from 0.94 – 190 × 10^4 M^{-1} (0.51 – 23 × 10^4 M^{-1}); in several cases the slope of the PSD is unity and therefore, the K_a values are too large to be measured by PSD techniques. The average K_{rel} value for **M2** versus **M2C2** toward a given drug is 6.6. The origins of this decrease in affinity of **M2C2** compared to **M2** is unclear although one can hypothesize that the location of the SO_3Na solubilizing groups close to the cavity of **M2C2** changes the aqueous solvation of the cavity which is known to provide a potent driving force in CB[n] complexation processes.[7f,27] Despite the decrease in slope observed for **M2C2** compared to **M2**, the concentration of drug that can be formulated with **M2C2** is often higher than can be achieved with **M2** as shown in Table 2. For example, the concentration of ethynylestradiol (33.6 versus 10.5 mM), camptothecin (28.3 versus 11.6 mM), and voriconazole (61.9 versus 9.23 mM) achieved with **M2C2** are substantially higher than with **M2**. These data suggest that **M2C2** has significant potential as a solubilizing excipient for insoluble drugs.

Binding Preferences of M2C2—Previously, we elucidated the binding preferences of acyclic CB[n]-type container **M2**.[21a] As expected based on its aromatic-CB[n] hybrid structure **M2** binds to hydrophobic or aromatic moieties in its cavity and cations at its portals. **M2** displays a special affinity for steroids. Analysis of the complexation induced changes in chemical shift for the 15 drugs with **M2C2** reveals similar preferences, namely cavity inclusion of the hydrophobic or aromatic moieties and portal binding of the cationic residues. Figure 6 shows the ^1H NMR recorded for 2-methoxyestradiol alone in DMSO because it is insoluble in D_2O, and in the presence of **M2** or **M2C2** in D_2O. The similar pattern of significant upfield shifts observed for the protons on the steroidal nucleus of 2-methoxyestradiol (s-bb) establish a similar binding mode within the acyclic CB[n] cavity defined by the naphthalene sidewalls.

Comparisons Among M1, M2, M2C2, HP-β-CD, and SBE-β-CD—Previously, we established that **M2** was a better solubilizing agent than **M1** and HP-β-CD according to PSD slope and K_{rel} values.[21a] Inspection of the PSDs for estradiol, voriconazole, and camptothecin (Figure 4) visually confirms that **M2C2** performs better as a solubilizing agent than either HP-β-CD or SBE-β-CD. The data given in Table 1 show that **M2C2** also performs better than HP-β-CD as a solubilizing agent for the remaining drugs in the test set with K_{rel} values ranging from a low of 1.5 to a high of 170 with an average of 10. The K_a values for HP-β-CD range from 0.016 – 3.6 × 10^4 M^{-1} whereas for **M2C2** they range from 0.51 – 51 × 10^4 M^{-1}. Several drugs (PBS-1086, camptothecin, aripiprazole) are nicely fomulated with **M2C2** where HP-β-CD is unsuccessful. It is also relevant to compare the

Author Manuscript Author Manuscript Author Manuscript Author Manuscript

solubilizing ability of **M2C2** versus highly soluble container **M1**[20a,21a] toward the insoluble drugs. Solubilization data is not available for 2-methoxyestradiol or MEPBZ with **M1**. Among the remaining 13 containers, **M2C2** is a better solubilizing agent than **M1** as judged by PSD slope toward 8 drugs, whereas **M2C2** and **M1** are comparable solubilizing agents for PBS-1086 and tamoxifen. In only three cases (melphalan, cinnarizine, albendazole) is **M1** more efficient than **M2C2**. The results given in Table 1 also establish that SBE-β-CD is a better solubilizing agent than HP-β-CD for all of the drugs tested in terms of PSD slope and K_a.[13e] The K_{rel} value for SBE-β-CD versus HP-β-CD ranges from a low of 1.9 to a high of 60. The anionic nature of SBE-β-CD makes it a better host for the drugs in the test set, many of which are cationic.[13e] A comparison between the solubilizing abilities of **M2C2** and SBE-β-CD is more subtle. In some cases (e.g. ethynylestradiol, tamoxifen) the slope of the PSD is substantially higher for SBE-β-CD whereas in other cases (cinnarizine, aripiprazole, voriconazole, 2-methoxyestradiol, MEPBZ) **M2C2** has a substantially larger slope. In several cases, the slopes are comparable (e.g. albendazole, amiodarone, estradiol). Significantly, **M2C2** – but not SBE-β-CD or HP-β-CD – was able to solubilize PBS-1086 and camptothecin. Table 2 gives the highest concentrations of drug that we achieved with **M2**, **M2C2**, and SBE-β-CD. For drugs where the slope of the PSD is significantly larger for SBE-β-CD (ethynylestradiol, tamoxifen), it is possible to prepare much higher drug concentrations due to the higher inherent solubility of SBE-β-CD (> 175 mM) relative to **M2C2**. Even in the case of voriconazole and amiodarone where the PSD slope is larger with **M2C2**, more concentrated solutions are ultimately obtained by using very high concentrations of SBE-β-CD. There are, however, situations where **M2C2** clearly performs better than SBE-β-CD (e.g. PBS-1086, camptothecin, MEPBZ) both in terms of PSD slope and maximum [drug].

In Vitro Cytotoxicity Assays

Given the very good performance of **M2C2** as a solubilizing agent for insoluble drugs, we wanted to take additional steps toward demonstrating the potential of **M2C2** in practical applications. Accordingly, we decided to perform a series of *in vitro* cytotoxicity assays to assess its biocompatibility. We elected to perform complementary cell viability (MTS) and cell cytolysis (Adenylate Kinase (AK) release) assays in human cell lines of kidney (HEK 293), human liver (HepG2), and human monocyte (THP-1) origin. As can be seen in Figure 7a,b,c the cells show decreases in cell viability (metabolic activity) at concentrations greater than 1 mM. In the complementary AK release assay no significant differences were noted between the untreated control cells and cells treated with up to 10 mM of **M2C2**. This result demonstrates that although at doses of 1 mM **M2C2** started to affect cell metabolism this did not lead to cell death. In combination, these results suggest that **M2C2** shows relatively low cytotoxicity toward the investigated cell lines.

Maximum Tolerated Dose Study

To assess the *in vivo* toxicity of **M2C2** we performed a maximal tolerated dose (MTD) study using outbred Swiss Webster mice. Mice were dosed daily *via* bolus injection of solvent, 475 mg kg^{-1} **M2C2**, or 950 mg kg^{-1} **M2C2** intraperitoneally for 14 consecutive days and then monitored for an additional two weeks for signs of sickness and weight change. Even at the

Author Manuscript Author Manuscript Author Manuscript Author Manuscript

maximal dose (950 mg/kg), the mice appeared healthy with no adverse reactions upon injection of the compound. Throughout the course of the study, the **M2C2** treated mice did not differ significantly in weight from the mice treated with solvent alone (20 mM phosphate buffer, pH 7.4). We conclude that **M2C2** displays no significant toxicity under the conditions of the MTD study.

Conclusions

In summary, we have reported the synthesis and characterization of **M2C2** and **M2C4** that are analogues of our previously reported **M2** container. Relative to **M2**, both **M2C2** and **M2C4** containers possess superior solubility in aqueous solution and do not undergo strong self-association processes that would impinge upon their function as solubilizing excipients for insoluble drugs. Container **M2C4** has a propensity to form gels both on its own at high concentrations and in the presence of drugs at lower concentrations. We constructed PSDs for the drugs in the test set for **M2C2** and SBE-β-CD to compare their solubilizing abilities. We find that **M2C2** and SBE-β-CD are complementary in that each container solubilizes some drugs better than the other in terms of both PSD slope and the maximum [drug]. In several cases **M2C2** and SBE-β-CD are comparable solubilizing agents. The results of *in vitro* cytotoxicity tests conducted using human kidney, liver, and monocyte cells demonstrate the good biocompatibility of **M2C2**. *In vivo* maximum tolerated dose studies in mice show that the animals tolerate **M2C2** at very high (950 mg kg^{-1}) doses. As a whole, this paper demonstrates that **M2C2** is an excellent solubilizing excipient for insoluble drugs that is in some cases comparable to SBE-β-CD which is used to formulate several drugs for administration to humans. In other cases (e.g. PBS-1086, camptothecin, MEPBZ) **M2C2** is clearly the better solubilizing agent. Comparison of the solubilizing ability of **M2C2** with **M1** shows that **M2C2** is as good or better than **M1** in 10 out of 13 cases. The work suggests that **M2C2** is a useful addition to the toolbox of solubilizing excipients to solve formulation challenges encountered by the pharmaceutical industry.

Experimental Section

Animal Studies

Animal studies were conducted at the University of Maryland, College Park, Maryland, USA, under the approval and guidance of Institutional Animal Care and Use Committee (IACUC; protocol #R-14-02).

Compound 2—1,4-Dihydroxynaphthalene (72 g, 0.45 mol), dibromoethane (400 mL, 4.64 mol), K_2CO_3 (250 g, 1.81 mol) and 18-crown-6 (5.77 g, 0.022 mol) were stirred in acetonitrile (400 mL) at 70°C, under nitrogen, for 3.5 days. The mixture was cooled to RT and filtered. The filtrate was concentrated by rotary evaporation. The crude solid was triturated with acetone (100 mL) and the solid was obtained by filtration. The solid was washed with the filtrate on the Büchner funnel, then with three portions of acetone (15 mL). The product was obtained as a white solid after drying under high vacuum (67 g, 40%). M.p. 126–128°C. IR (ATR, cm^{-1}): 3438w, 2892w, 1592m, 1270s, 1099s, 766s. ^{1}H NMR (500 MHz, $CDCl_3$): 8.28–8.27 (m, 2H), 7.56–7.54 (m, 2H), 6.68 (s, 2H), 4.41 (t, J = 6 Hz, 4H),

Author Manuscript Author Manuscript Author Manuscript Author Manuscript

3.76 (t, J = 6 Hz, 4H). ^{13}C NMR (125 MHz, $CDCl_3$): 148.6, 126.7, 126.4, 122.0, 105.1, 68.7, 29.6.

Compound 3—A solution of **2** (40.2 g, 107.5 mmol) and Na_2SO_3 (29.8 g, 236.4 mmol) in H_2O/DMF (1:1, 400 mL) under N_2 were stirred at 100°C for 24 h. The mixture was cooled to RT and filtered. The filtrate was poured into acetone (2 L) and the precipitate was obtained by filtration and dried on the filter funnel overnight. The crude solid was dissolved in boiling water (86 mL) and then EtOH (250 mL) was added to precipitate the product. The mixture was cooled to room temperature, filtered and the product was obtained as a white solid after drying under high vacuum (36.7 g, 81%). M.p.>300°C (dec.). IR (ATR, cm^{-1}): 3438w, 2941w, 1595w, 1200s, 1043s, 767m. ^{1}H NMR (400 MHz, D_2O): 8.28–8.26 (m, 2H), 7.62–7.59 (m, 2H), 7.00 (s, 2H), 4.54 (t, J = 6 Hz, 4H), 3.50 (t, J = 6 Hz, 4H). ^{13}C NMR (125 MHz, D_2O, dioxane as reference): 151.0, 129.3, 129.0, 124.6, 109.2, 69.5, 53.4. Low-Resolution MS (ESI): *m/z* 375 ([M+H-2Na] $^-$, calculated for $C_{14}H_{15}O_8S_2^-$: 375).

Container M2C2—To a solution of **6**[28] (7.49 g, 9.59 mmol) in TFA/Ac_2O (1:1, 90 mL) was added **3** (12.1 g, 28.78 mmol) and the mixture was stirred at 70°C for 2 h, under nitrogen. The mixture was cooled to RT and poured into 700 mL of EtOH. The solid was filtered and washed on the filter funnel with three portions of EtOH (150 mL) and then dried on the filter funnel. The crude solid was dissolved in 250 mL of water and the pH was adjusted to pH 7 with a concentrated NaOH solution. Acetonitrile (1.1 L) was added to the aqueous solution to precipitate the product. The solid was filtered. The solid was dissolved in boiling water (100 mL), then acetonitrile (300 mL) was added and the mixture was cooled to RT. The product was obtained by filtration after drying under high vacuum as a white solid (8.77 g, 58%). M.p.>300°C. IR (ATR, cm^{-1}): 3349w, 2941w, 1722s, 1468s, 1172s, 1033s, 798m. ^{1}H NMR (600 MHz, D_2O): 7.72–7.71 (m, 4H), 7.04–7.02 (m, 4H), 5.51 (d, J = 16 Hz, 4H), 5.50 (d, J = 15 Hz, 2H), 5.37 (d, J = 16 Hz, 4H), 5.35 (d, J = 9 Hz, 2H), 5.24 (d, J = 9 Hz, 2H), 4.54 (d, J = 16 Hz, 4H), 4.46–4.42 (m, 4H), 4.19 (d, J = 16 Hz, 4H), 4.19–4.15 (m, 4H), 3.94 (d, J = 15 Hz, 2H), 3.49 (t, J = 7 Hz, 8H), 1.78 (s, 6H), 1.77 (s, 6H). ^{13}C NMR (125 MHz, D_2O, dioxane as reference): 158.5, 157.6, 150.0, 129.5, 129.4, 128.6, 124.5, 80.4, 79.1, 73.4, 73.2, 72.1, 55.0, 52.7, 50.5, 38.0, 17.4, 16.8. HR-MS (ESI): *m/z* 769.1329 ([M-2Na]$^{2-}$, calculated for $C_{58}H_{60}N_{16}Na_2O_{24}S_4^{2-}$: 769.1328).

Compound 5—A solution of 1,4-butanesultone (13.04 g, 96 mmol) in 1,4-dioxane (79 mL) was added to a solution of 1,4-dihydroxynaphtalene (6.14 g, 38 mmol) and NaOH (4.9 g, 123 mmol) in water (49 mL). The mixture was stirred at RT for 12 h. MeOH (200 mL) was added to the solution and the precipitate was isolated by filtration. The solid was dissolved in water (35 mL) and re-precipitated by addition of EtOH (70 mL). After filtration and drying under high vacuum, the product (**5**) was obtained as a light gray solid (4.69 g, 26%). M.p.>300°C (dec.). IR (ATR, cm^{-1}): 3417w, 2922w, 1594w, 1185s, 1040s, 768m. ^{1}H NMR (400 MHz, D_2O): 8.25–8.22 (m, 2H), 7.62–7.59 (m, 2H), 6.97 (s, 2H), 4.22 (t, J = 5.5 Hz, 4H), 3.02 (t, J = 7.5 Hz, 4H), 2.02–1.99 (m, 8H). ^{13}C NMR (125 MHz, D_2O, dioxane as reference): 148.7, 126.9, 126.6, 122.1, 106.8, 69.2, 51.5, 28.2, 21.9. Low-Resolution MS (ESI): *m/z* 215 ([M-2Na]$^{2-}$, calculated for $C_{18}H_{22}O_8S_2^{2-}$: 215).

Author Manuscript Author Manuscript Author Manuscript Author Manuscript

Container M2C4—To a solution of **6**[28] (1.14 g, 1.46 mmol) in TFA/Ac_2O (1:1, 14 mL) was added **5** (2.40 g, 5.04 mmol) and the mixture was stirred at 70 °C for 3 h, under nitrogen. The reaction mixture was cooled to RT and poured into EtOH (100 mL). The crude solid was obtained by filtration and dried on the filter funnel. The crude solid was dissolved in water (10 mL) and the pH was adjusted to pH 7 with a concentrated NaOH solution. EtOH (40 mL) was added to the boiling aqueous solution to precipitate the product and the mixture was cooled to RT. The solid was obtained by filtration. The crude solid was dissolved in boiling water (5 mL) and then reprecipitated by the addition of EtOH (5 mL) and the mixture was cooled to RT and the solid was obtained by filtration. A second re-precipitation under the same conditions delivered the product as a white solid after drying under high vacuum (1.06 g, 43%). M.p.>300°C. IR (ATR, cm^{-1}): 3438w, 2942w, 1722s, 1468s, 1177s, 1036s, 798m. ^1H NMR (400 MHz, D_2O): 7.90–7.88 (m, 4H), 7.47–7.45 (m, 4H), 5.54 (d, J = 15 Hz, 2H), 5.51 (d, J = 16 Hz, 4H), 5.40 (d, J = 9 Hz, 2H), 5.38 (d, J = 16 Hz, 4H), 5.29 (d, J = 9 Hz, 2H), 4.42 (d, J = 16 Hz, 4H), 4.24 (d, J = 16 Hz, 4H), 4.10–4.05 (m, 4H), 4.00 (d, J = 15 Hz, 2H), 3.85–3.80 (m, 4H), 2.93–2.77 (m, 8H), 1.96–1.86 (m, 8H), 1.86–1.71 (m, 8H), 1.76 (s, 12H). ^{13}C NMR (125 MHz, D_2O, dioxane as reference): 158.5, 157.7, 150.2, 129.7, 129.2, 128.5, 124.5, 80.5, 79.2, 77.3, 73.4, 73.1, 54.9, 52.8, 50.5, 38.1, 30.4, 23.0, 17.4, 16.9. HR-MS (ESI): *m/z* 825.1954 ($[M-2Na]^{2-}$, calculated for $C_{66}H_{76}N_{16}Na_2O_{24}S_4^{2-}$: 825.1954).

Supplementary Material

Refer to Web version on PubMed Central for supplementary material.

Acknowledgments

We thank the National Institutes of Health (CA168365) for financial support of this work. Shane Falcinelli was supported by an HHMI undergraduate research fellowship. We thank Dr. Xiaoyong Lu for performing mass spectrometric measurements.

References

1. a) Pluth MD, Raymond KN. Chem Soc Rev. 2007; 36:161–171. [PubMed: 17264920] b) Northrop BH, Zheng YR, Chi KW, Stang PJ. Acc Chem Res. 2009; 42:1554–1563. [PubMed: 19555073] c) Diederich F. Angew Chem. Intl Ed Engl. 1988; 27:362–386.d) Cram DJ. Angew Chem. Int Ed Engl. 1988; 27:1009–1020.e) Lehn JM. Angew Chem. Int Ed Engl. 1988; 27:89–112.f) Ogoshi T, Kanai S, Fujinami S, Yamagishi TA, Nakamoto Y. J Am Chem Soc. 2008; 130:5022–5023. [PubMed: 18357989] g) Masson E, Ling X, Joseph R, Kyeremeh-Mensah L, Lu X. RSC Adv. 2012; 2:1213–1247.h) Gutsche CD. Acc Chem Res. 1983; 16:161–170.i) Boehmer V. Angew Chem. Int Ed Engl. 1995; 34:713–745.j) Rekharsky MV, Inoue Y. Chem Rev. 1998; 98:1875–1917. [PubMed: 11848952] k) Barnes JC, Juricek M, Strutt NL, Frasconi M, Sampath S, Giesener MA, McGrier PL, Bruns CJ, Stern CL, Sarjeant AA, Stoddart JF. J Am Chem Soc. 2012; 135:183–192. [PubMed: 22928610] l) Rebek J. Acc Chem Res. 2009; 42:1660–1668. [PubMed: 19603810] m) Xue M, Yang Y, Chi X, Zhang Z, Huang F. Acc Chem Res. 2012; 45:1294–1308. [PubMed: 22551015] n) Kay ER, Leigh DA. Angew Chem. Int Ed. 2015; 54:10080–10088.o) Hermann K, Ruan Y, Hardin AM, Hadad CM, Badjic JD. Chem Soc Rev. 2015; 44:500–514. [PubMed: 24927358] p) Lin Z, Emge TJ, Warmuth R. Chem - Eur J. 2011; 17:9395–9405. [PubMed: 21735498] q) Zarra S, Wood DM, Roberts DA, Nitschke JR. Chem Soc Rev. 2015; 44:419–432. [PubMed: 25029235] r) Yoshizawa M, Klosterman J, Fujita M. Angew Chem. Int Ed. 2009; 48:3418–3438.

2. Mal P, Breiner B, Rissanen K, Nitschke JR. Science. 2009; 324:1697–1699. [PubMed: 19556504]

Author Manuscript Author Manuscript Author Manuscript Author Manuscript

3. Juricek M, Strutt NL, Barnes JC, Butterfield AM, Dale EJ, Baldridge KK, Stoddart JF, Siegel JS. Nat Chem. 2014; 6:222–228. [PubMed: 24557137]
4. Pluth MD, Bergman RG, Raymond KN. Science. 2007; 316:85–88. [PubMed: 17412953]
5. You L, Zha D, Anslyn EV. Chem Rev. 2015; 115:7840–7892. [PubMed: 25719867]
6. a) Liu S, Russell DH, Zinnel NF, Gibb BC. J Am Chem Soc. 2013; 135:4314–4324. [PubMed: 23448338] b) Ajami D, Liu L, Rebek J Jr. Chem Soc Rev. 2015; 44:490–499. [PubMed: 24705709]
7. a) Mock WL, Shih NY. J Org Chem. 1986; 51:4440–4446.b) Liu S, Ruspic C, Mukhopadhyay P, Chakrabarti S, Zavalij PY, Isaacs L. J Am Chem Soc. 2005; 127:15959–15967. [PubMed: 16277540] c) Cao L, Šekutor M, Zavalij PY, Mlinaricć-Majerski K, Glaser R, Isaacs L. Angew Chem. Int Ed. 2014; 53:988–993.d) Isaacs L. Acc Chem Res. 2014; 47:2052–2062. [PubMed: 24785941] e) Moghaddam S, Yang C, Rekharsky M, Ko YH, Kim K, Inoue Y, Gilson MK. J Am Chem Soc. 2011; 133:3570–3581. [PubMed: 21341773] f) Biedermann F, Uzunova VD, Scherman OA, Nau WM, De Simone A. J Am Chem Soc. 2012; 134:15318–15323. [PubMed: 22881280] g) Shetty D, Khedkar JK, Park KM, Kim K. Chem Soc Rev. 2015; 44:8747–8761. [PubMed: 26434388]
8. a) Mock WL, Irra TA, Wepsiec JP, Adhya M. J Org Chem. 1989; 54:5302–5308.b) Pemberton BC, Raghunathan R, Volla S, Sivaguru J. Chem Eur J. 2012; 18:12178–12190. [PubMed: 22945866] c) Zheng L, Sonzini S, Ambarwati M, Rosta E, Scherman OA, Herrmann A. Angew Chem. Int Ed. 2015; 54:13007–13011.d) Jon SY, Ko YH, Park SH, Kim HJ, Kim K. Chem Commun. 2001 1938–1939.
9. a) Dsouza R, Hennig A, Nau W. Chem Eur J. 2012; 18:3444–3459. [PubMed: 22367854] b) Ghale G, Lanctot AG, Kreissl HT, Jacob MH, Weingart H, Winterhalter M, Nau WM. Angew Chem. Int Ed. 2014; 53:2762–2765.c) Gong B, Choi BK, Kim JY, Shetty D, Ko YH, Selvapalam N, Lee NK, Kim K. J Am Chem Soc. 2015; 137:8908–8911. [PubMed: 26160008]
10. a) Barrow SJ, Kasera S, Rowland MJ, del Barrio J, Scherman OA. Chem Rev. 2015; 115:12320–12406. [PubMed: 26566008] b) Dang D, Nguyen H, Merkx M, Brunsveld L. Angew Chem. Int Ed. 2013; 52:2915–2919.c) Walsh Z, Janecek ER, Hodgkinson JT, Sedlmair J, Koutsioubas A, Spring DR, Welch M, Hirschmugl CJ, Toprakcioglu C, Nitschke JR, Jones M, Scherman OA. Proc Natl Acad Sci U S A. 2014; 111:17743–17748. [PubMed: 25385610]
11. a) Lim S, Kim H, Selvapalam N, Kim KJ, Cho SJ, Seo G, Kim K. Angew Chem Int Ed. 2008; 47:3352–3355.b) Tian JA, Ma SQ, Thallapally PK, Fowler D, McGrail BP, Atwood JL. Chem Commun. 2011; 47:7626–7628.c) Miyahara Y, Abe K, Inazu T. Angew Chem. Int Ed. 2002; 41:3020–3023.
12. a) Hauss DJ. Adv Drug Delivery Rev. 2007; 59:667–676.b) Lipinski CA. J Pharmacol Toxicol Methods. 2000; 44:235–249. [PubMed: 11274893]
13. a) Leuner C, Dressman J. Eur J Pharmaceut Biopharmaceut. 2000; 50:47–60.b) Muller RH, Keck CM. J Biotechnol. 2004; 113:151–170. [PubMed: 15380654] c) Serajuddin ATM. Adv Drug Delivery Rev. 2007; 59:603–616.d) Stella VJ, Nti-Addae KW. Adv Drug Delivery Rev. 2007; 59:677–694.e) Okimoto K, Rajewski RA, Uekama K, Jona JA, Stella VJ. Pharm Res. 1996; 13:256–264. [PubMed: 8932446] f) Stella VJ, Rajewski RA. Pharm Res. 1997; 14:556–567. [PubMed: 9165524]
14. a) Ghosh I, Nau WM. Adv Drug Delivery Rev. 2012; 64:764–783.b) Dong N, Wang X, Pan J, Tao Z. Acta Chim Sinica. 2011; 69:1431–1437.c) Walker S, Oun R, McInnes FJ, Wheate NJ. Isr J Chem. 2011; 51:616–624.d) Zhao Y, Buck DP, Morris DL, Pourgholami MH, Day AI, Collins JG. Org Biomol Chem. 2008; 6:4509–4515. [PubMed: 19039358]
15. a) Uzunova VD, Cullinane C, Brix K, Nau WM, Day AI. Org Biomol Chem. 2010; 8:2037–2042. [PubMed: 20401379] b) Hettiarachchi G, Nguyen D, Wu J, Lucas D, Ma D, Isaacs L, Briken V. PLoS One. 2010; 5:e10514. [PubMed: 20463906]
16. a) Chen H, Y-W CJ, Li S, Liu JJ, Wyman I, Lee SM-Y, Macartney DH, Wang R. RSC Adv. 2015; 5:63745–63752.b) Li S, Chen H, Yang X, Bardelang D, Wyman IW, Wan J, Lee SMY, Wang R. ACS Med Chem Lett. 2015; 6:1174–1178. [PubMed: 26713100]
17. Zhang J, Coulston RJ, Jones ST, Geng J, Scherman OA, Abell C. Science. 2012; 335:690–694. [PubMed: 22323815]

Author Manuscript Author Manuscript Author Manuscript Author Manuscript

18. a) Cao L, Hettiarachchi G, Briken V, Isaacs L. Angew Chem. Int Ed. 2013; 52:12033–12037.b) Kim E, Kim D, Jung H, Lee J, Paul S, Selvapalam N, Yang Y, Lim N, Park CG, Kim K. Angew Chem. Int Ed. 2010; 49:4405–4408.
19. a) Huang WH, Zavalij PY, Isaacs L. J Am Chem Soc. 2008; 130:8446–8454. [PubMed: 18529059] b) Lucas D, Minami T, Iannuzzi G, Cao L, Wittenberg JB, Anzenbacher P, Isaacs L. J Am Chem Soc. 2011; 133:17966–17976. [PubMed: 21970313]
20. a) Ma D, Hettiarachchi G, Nguyen D, Zhang B, Wittenberg JB, Zavalij PY, Briken V, Isaacs L. Nat Chem. 2012; 4:503–510. [PubMed: 22614387] b) Hettiarachchi G, Samanta S, Falcinelli S, Zhang B, Moncelet D, Isaacs L, Briken V. Mol Pharmaceut. 201610.1021/acs.molpharmaceut.1025b00723
21. a) Zhang B, Isaacs L. J Med Chem. 2014; 57:9554–9563. [PubMed: 25369565] b) Gilberg L, Zhang B, Zavalij PY, Sindelar V, Isaacs L. Org Biomol Chem. 2015; 13:4041–4050. [PubMed: 25731639]
22. CCDC-1452394 (**M2C4**) contains the supplementary crystallographic data for this paper. These data can be obtained free of charge from the cambridge crystallographic data centre via http://www.Ccdc.Cam.Ac.Uk/data_request/cif
23. a) Higuchi T, Connors KA. Adv Anal Chem Inst. 1965; 4:117–212.b) Connors, KA. Binding constants. John Wiley & Sons; New York: p. 1987
24. Fabre C, Mimura N, Bobb K, Kong SY, Gorgun G, Cirstea D, Hu J, Minami J, Ohguchi H, Zhang J, Meshulam J, Carrasco RD, Tai YT, Richardson PG, Hideshima T, Anderson KC. Clin Cancer Res. 2012; 18:4669–4681. [PubMed: 22806876]
25. Mandadapu, V. PhD dissertation. University of New South Wales; Canberra, Australia: 2014.
26. a) Ma D, Zhang B, Hoffmann U, Sundrup MG, Eikermann M, Isaacs L. Angew Chem. Int Ed. 2012; 51:11358–11362.b) Hoffmann U, Grosse-Sundrup M, Eikermann-Haerter K, Zaremba S, Ayata C, Zhang B, Ma D, Isaacs L, Eikermann M. Anesthesiology. 2013; 119:317–325. [PubMed: 23549405] c) Haerter F, Simons JCP, Foerster U, Duarte IM, Diaz-Gil D, Eikermann-Haerter K, Ayata C, Ganapati S, Zhang B, Blobner M, Isaacs L, Eikermann M. Anesthesiology. 2015; 123:1337–1349. [PubMed: 26418697]
27. Biedermann F, Nau WM, Schneider HJ. Angew Chem. Int Ed. 2014; 53:11158–11171.
28. Ma D, Zavalij PY, Isaacs L. J Org Chem. 2010; 75:4786–4795. [PubMed: 20540586]

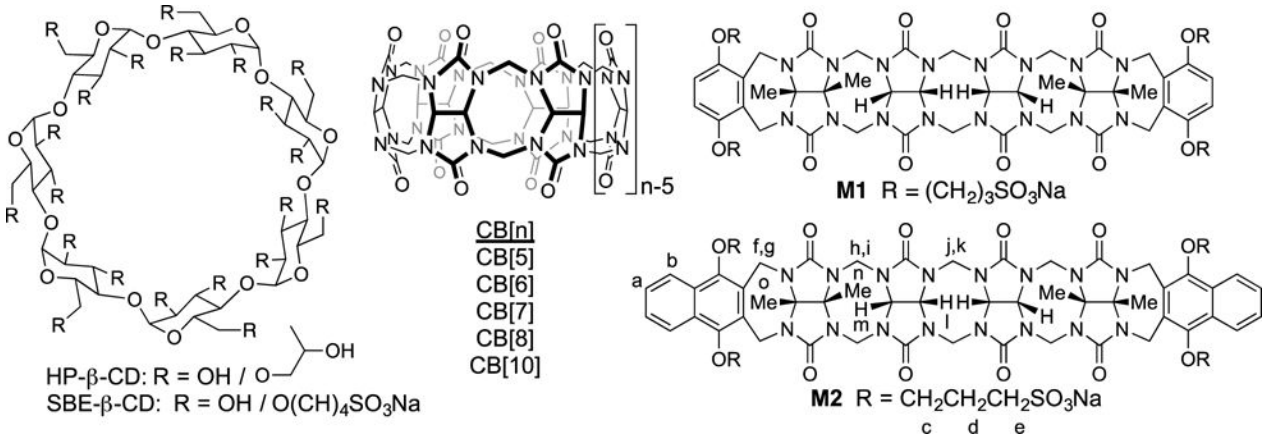

Figure 1.

Chemical structures of HP-β-CD (average degree of substitution = 4.9), SBE-β-CD (average degree of substitution = 6.5), CB[n], **M1** and **M2** that have previously been used as solubilizing excipients for insoluble drugs.

Author Manuscript Author Manuscript Author Manuscript Author Manuscript

Author Manuscript Author Manuscript Author Manuscript Author Manuscript

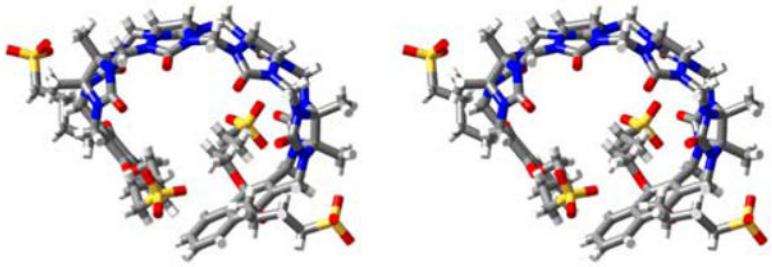

Figure 2.
Cross-eyed stereoview of one molecule of **M2C4** in the crystal. Color code: C, grey; H, white; N, blue; O, red; S, yellow; H-bonds, red-yellow stripped.

Author Manuscript Author Manuscript Author Manuscript Author Manuscript

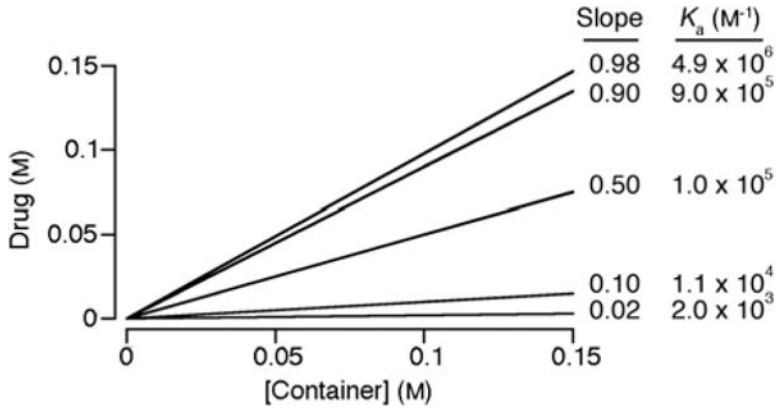

Figure 3.

Simulated PSDs for container•drug systems that obey equation 1 with S_0 = 10 μM, different values of slope and the corresponding values of K_a.

Author Manuscript Author Manuscript Author Manuscript Author Manuscript

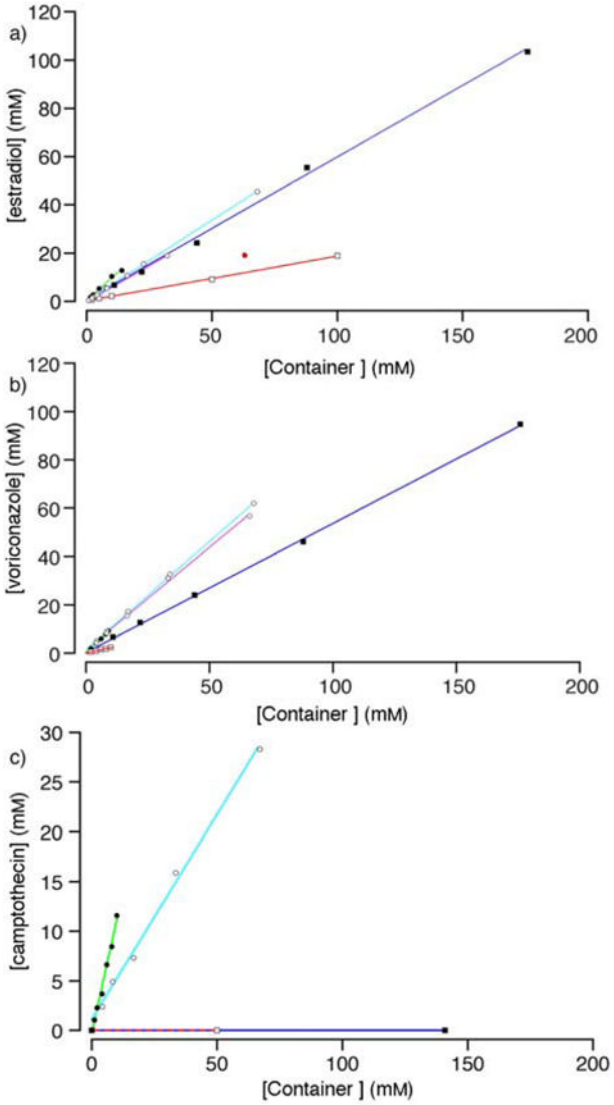

Figure 4.

PSDs constructed from the solubilization data for: a) estradiol, b) voriconazole, c) camptothecin with different containers (**M2**, ●; **M2C2**, o; **M2C4**, ⊙; HP-β-CD, □; SBE-β-CD, ■. Conditions: 20 mM sodium phosphate buffered D_2O (pD = 7.4, rt). Data points colored red were not used in the linear regression.

Author Manuscript Author Manuscript Author Manuscript Author Manuscript

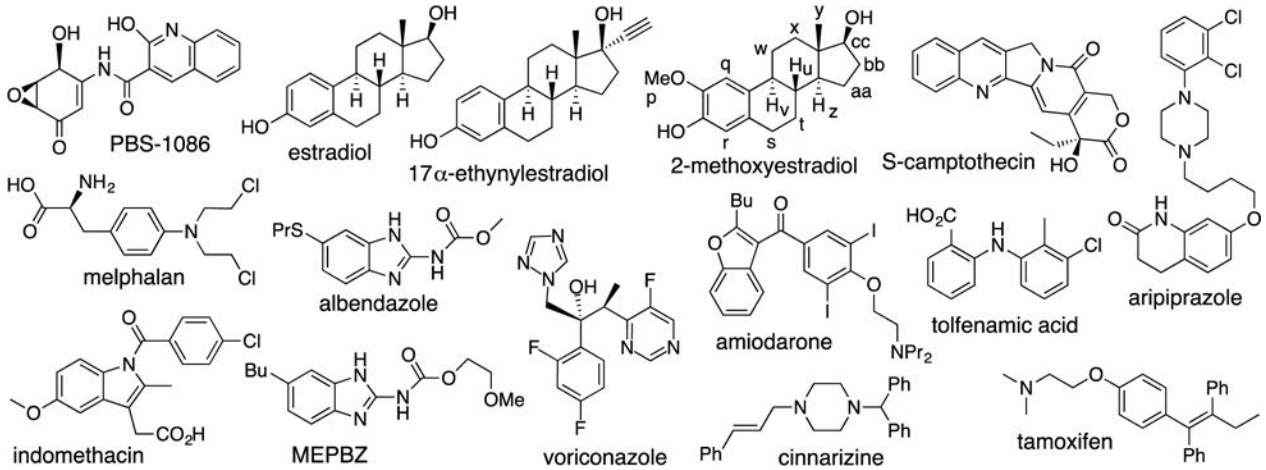

Figure 5.
Chemical structures of the 15 insoluble drugs studied in this paper.

Author Manuscript Author Manuscript Author Manuscript Author Manuscript

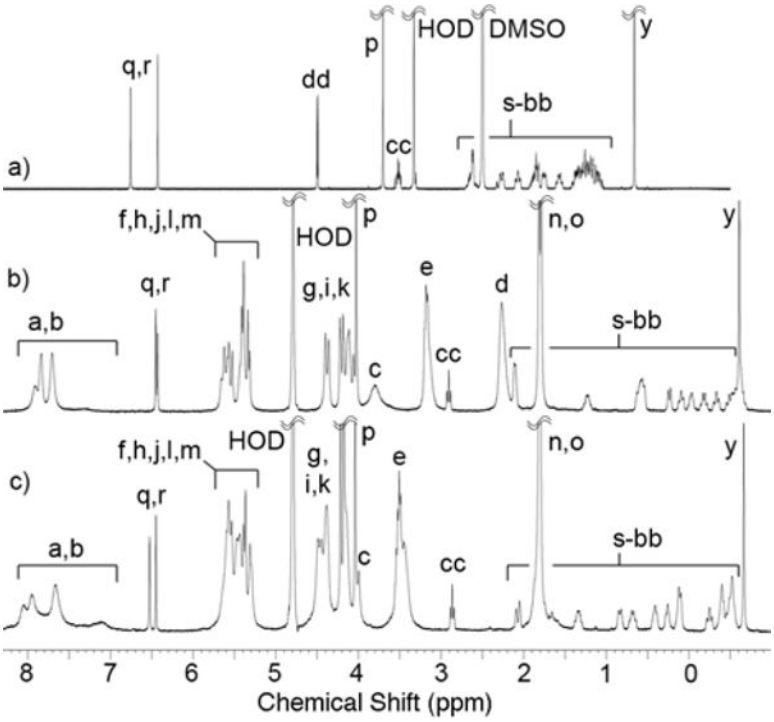

Figure 6.

^{1}H NMR spectra recorded (400 MHz, RT) for 2-methoxyestradiol: a) alone in DMSO-d_6, or b) with **M2**, or c) with **M2C2** in 20 mM sodium phosphate buffered D_2O at pD 7.4.

Author Manuscript Author Manuscript Author Manuscript Author Manuscript

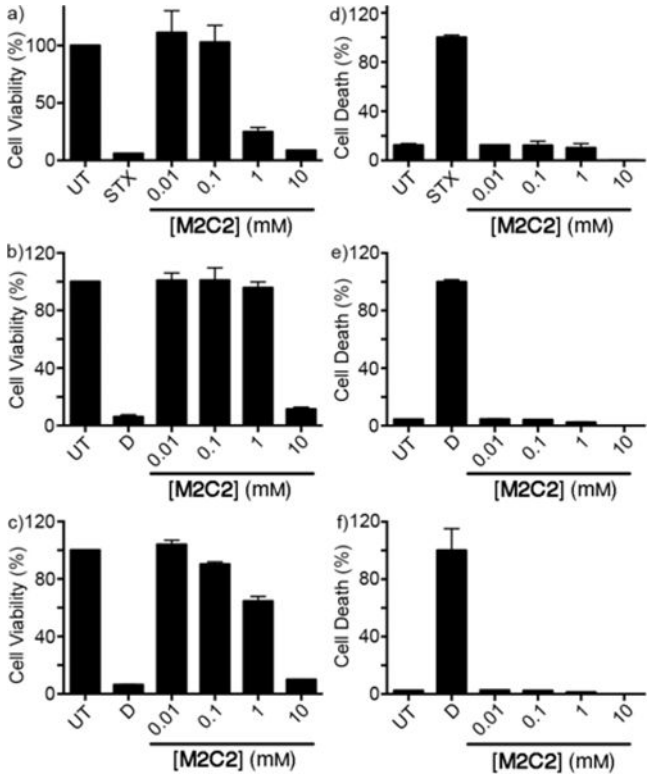

Figure 7.

In vitro toxicology of **M2C2**. MTS (a, b, c) and AK release assay (d, e, f) were performed to evaluate the cell viability and the cell death of three cell lines treated with **M2C2**. THP-1 (a, d), HepG2 (b, e) and HEK293 (c, f). UT = untreated cells, STX = Staurosporine, D = Distilled water. Representative data from two independent experiments performed in triplicate. Error bars represent the standard deviation. Cells were treated with solutions of **M2C2** for 24 hours.

Author Manuscript Author Manuscript Author Manuscript Author Manuscript

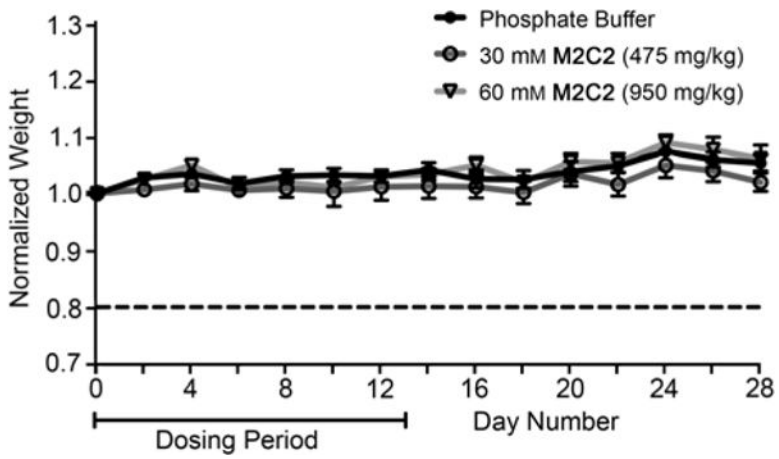

Figure 8.

Female Swiss Webster mice (n = 7 per group) were dosed intraperitoneally with solvent (phosphate buffer), 475 mg/kg **M2C2**, or 950 mg/kg **M2C2** for 14 consecutive days. Weight change is represented as the group average (n = 7) of mouse weight at day n to weight at day 0. Error bars represent standard error of the mean.

Author Manuscript Author Manuscript Author Manuscript Author Manuscript

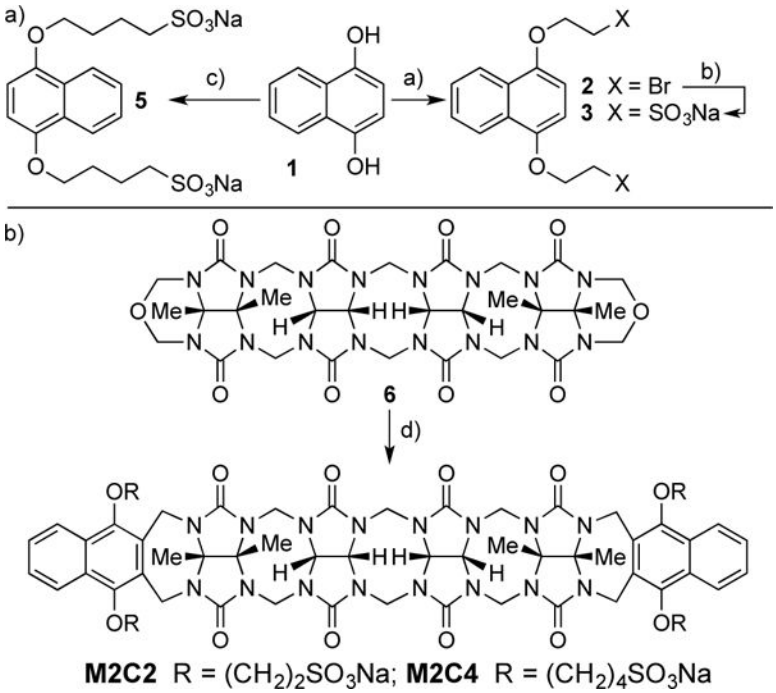

Scheme 1.

Synthesis of: a) aromatic walls **3** and **5**, and b) acyclic CB[n]-type molecular containers **M2C2** and **M2C4**. Conditions: a) K_2CO_3, 18-crown-6, $BrCH_2CH_2Br$, CH_3CN, 70 °C; b) Na_2SO_3 in H_2O/DMF (1:1),100 °C, 81%; c) butanesultone (**4**), NaOH, H_2O, dioxane, RT, 26%; d) CF_3CO_2H/Ac_2O (1:1), 70 °C, (**M2C2**, 58%; **M2C4** 43%).

Author Manuscript Author Manuscript Author Manuscript Author Manuscript

Table 1

Parameters from the phase solubility diagrams.

		Initial slope of the PSD					K_{rel}/K_a*10^4 (M^{-1})				
Drug	**S_0 (μM)**	**HP-β-CD**	**SBE-β-CD**	**M2**	**M2C2**	**M2C4**	**HP-β-CD[20a,21a]**	**SBE-β-CD**	**M2[20a,21a]**	**M2C2**	**M2C4**
PBS-1086	4.5	0	0	0.89	0.70	n.d.	–	–	3.5/190	1/51	n.d.
Ethynyl Estradiol	24	0.47	0.93	1.1	0.57	n.d.	1/3.6	14/53	TL/TL	1.5/5.5	n.d.
Camptothecin	54	0	0	1.1	0.41	n.d.	–	–	TL/TL	1/1.3	n.d.
Cinnarizine	14	0.002	0.008	0	0.26	n.d.	1/0.016	4.0/0.058	–	170/2.5	n.d.
Albendazole	2.7	0.015	0.027	0.48	0.035	n.d.	1/0.54	1.9/1.1	62/34	2.4/1.4	n.d.
Estradiol	8.8	0.18	0.59	0.92	0.67	0.59	1/2.6	6.7/17	51/130	9.1/23	6.5/16
Amiodarone	66	0.089	0.60	1.03	0.65	Gel	1/0.15	15/2.3	TL/TL	19/2.8	n.d.
Indomethacin	5.7	0.013	0.23	0.47	0.13	n.d.	1/0.24	22/5.1	67/16	11/2.5	n.d.
Aripiprazole	23	0	0.048	0.31	0.28	n.d.	–	1.0/0.22	8.8/2.0	7.7/1.7	n.d.
Melphalan	n.d.	0.11	0.50	1.1	0.43	n.d.	1/–	8/–	TL/–	6.0/–	n.d.
Voriconazole	38	0.22	0.53	1.0	0.89	0.85	1/0.76	4.0/3.0	TL/TL	29/21	19/14
Tamoxifen	12	0.028	0.63	0.10	0.058	n.d.	1/0.24	60/14	3.9/0.94	2.1/0.51	n.d.
Tolfenamic acid	1.9	0.0080	0.11	0.54	0.11	n.d.	1/0.41	15/6.4	150/63	16/6.6	n.d.
2-Methoxy estradiol	n.d.	0.074	0.21	0.79	0.49	n.d.	1/–	3.3/–	47/–	12/–	n.d.
MEPBZ	1.4	0.024	0.046	0.53	0.28	n.d.	1/1.8	1.9/3.5	46/82	15/28	n.d.

n.d., not determined; –, cannot be calculated because slope = 0 or S_0 was not determined; TL, too large to be determined because slope ≈ 1.

Author Manuscript

Author Manuscript

Author Manuscript

Author Manuscript

Table 2

Highest drug concentrations (mM) achieved with each container.

Drug	M2	M2C2	SBE-β-CD
PBS-1086	12.5	16.5	0
Ethynylestradiol	10.5	33.6	131
Camptothecin	11.6	28.3	0
Cinnarizine	0	4.40	1.71
Albendazole	4.48	2.78	3.94
estradiol	12.9	45.6	103
amiodarone	5.1	31.4	75.1
Indomethacin	6.70	6.69	9.92
Aripiprazole	3.20	9.26	8.44
Melphalan	16.1	38.2	87.8
Voriconazole	9.23	61.9	94.7
Tamoxifen	1.18	3.72	71.8
Tolfenamic acid	5.6	6.79	8.07
2-methoxyestradiol acid	6.42	34.1	35.9
MEPBZ	5.07	20	5.54